Three-Dimensional Structure of Chymotrypsin Inactivated with (2*S*)-*N*-Acetyl-L-alanyl-L-phenylalanyl α-chloroethane: Implications for the Mechanism of Inactivation of Serine Proteases by Chloroketones[†,‡]

Kevin Kreutter,[§] Anke C. U. Steinmetz,[∥] Tzyy-Chyau Liang,[⊥,#] Maryfrances Prorok,[⊥,△] Robert H. Abeles,[⊥] and Dagmar Ringe[*,⊥,▽,○]

Departments of Biochemistry and Chemistry, Programs in Bioorganic Chemistry and Biophysics, and Rosenstiel Basic Medical Sciences Research Center, Brandeis University, Waltham, Massachusetts 02254

Received May 27, 1994; Revised Manuscript Received September 7, 1994[⊗]

ABSTRACT: The reaction of enantiomerically pure (2*S*)-*N*-acetyl-L-alanyl-L-phenylalanyl α-chloroethane with γ-chymotrypsin was studied as a probe of the mechanism of inactivation of serine proteases by peptidyl chloroalkanes. It was determined crystallographically that the peptidyl chloroethane alkylates His57 with retention of configuration at the chiral center, indicating a double displacement mechanism. We think it likely that a Ser195−epoxy ether adduct is an intermediate on the inactivation pathway, although other possibilities have not been disproven. Kinetic data reported by others [Angliker et al. (1988) *Biochem. J. 256,* 481−486] indicate that the epoxy ether intermediate is not an irreversibly inactivated form of enzyme [a conclusion confirmed experimentally (Prorok et al. (1994) *Biochemistry 33,* 9784−9790)] and that both ring closure of the tetrahedral intermediate to form the epoxy ether and ring opening by His57 partially limit the first-order rate constant for inactivation, k_i. The peptidyl chloroethyl derivative adopts a very different active site conformation from that assumed by serine proteases inactivated by peptidyl chloromethanes. Positioning the chloroethyl derivative into the conformation adopted by chloromethyl derivatives would cause the extra methyl group to make a bad van der Waals contact with the inactivator P_2 carbonyl carbon, thereby preventing the formation of the invariant hydrogen bond between the inactivator P_1 amide nitrogen and the carbonyl group of Ser214. We conclude that the unusual conformation displayed by the chloroethyl derivative is caused by steric hindrance between the extra methyl group and the rest of the inactivator chain.

Peptidyl chloromethanes, such as L-1-(tosylamino)-2-phenylethyl chloromethyl ketone (TPCK),[1] are regarded as affinity labels of serine proteases which alkylate His57 of chymotrypsin (Powers, 1977). Currently, they find use in identifying and inactivating specific proteases *in vitro* (Angliker et al., 1993) and in living cells (Hallenberger et al., 1992). The simplest mechanism for inactivation involves the reversible formation of a Michaelis complex between the enzyme and the inactivator, followed by nucleophilic displacement of the chloride anion by His57. This was shown to be *too* simple when it was discovered that anhydrochymotrypsin (lacking the nucleophilic hydroxyl group of Ser195) was not alkylated by peptidyl chloromethanes, even though it could bind substrates with affinities comparable to that for native chymotrypsin (Weiner et al., 1966). This result, implicating Ser195 in the mechanism of inactivation, is supported by X-ray crystallographic (Scott et al., 1986; Banner & Hadvary, 1991, and references cited therein) and ^{13}C NMR (Finucane & Malthouse, 1992, and references cited therein) studies of trypsin, *Streptomyces griseus* protease B, thrombin, and elastase, which invariably show a Ser195−hemiketal adduct with the P_1[2] carbonyl group of the methyl ketone in addition to His alkylation at the methylene carbon. This covalent Ser195 linkage has also been confirmed in crystallographic studies of peptidyl chloromethane-inactivated chymotrypsin and subtilisin where the hemiketal moiety initially escaped notice (Poulos et al., 1976).

[†] This project is supported in part by a grant from the Lucille P. Markey Charitable Trust and in part by the Bioorganic Chemistry Program Training Grant at Brandeis University (NIH 1 T32GM08417-01). K.K. is supported by a National Science Foundation Pre-Doctoral Fellowship.

[‡] Atomic coordinates have been deposited in the Brookhaven Protein Data Bank, entry 2GMT.

* To whom correspondence should be addressed.

[§] Program in Bioorganic Chemistry.

[∥] Program in Biophysics.

[⊥] Department of Biochemistry.

[#] Present address: Department of Biochemistry and Molecular Biology, University of Texas Medical School, Houston, TX 77225.

[△] Present address: Department of Chemistry and Biochemistry, University of Notre Dame, South Bend, IN 46556.

[▽] Department of Chemistry.

[○] Rosenstiel Basic Medical Sciences Research Center.

[⊗] Abstract published in *Advance ACS Abstracts,* October 15, 1994.

[1] Abbreviations: TPCK, L-1-(tosylamino)-2-phenylethyl chloromethyl ketone; AcAFCEK, *N*-acetyl-L-alanyl-L-phenylalanyl α-chloroethane; (D)FPRCMK, D-phenylalanyl-L-prolyl-L-arginyl chloromethane; (D)FPRFMK, D-phenylalanyl-L-prolyl-L-arginyl fluoromethane; AFKCMK, L-alanyl-L-phenylalanyl-L-lysyl chloromethane; AFKFMK, L-alanyl-L-phenylalanyl-L-lysyl fluoromethane; Boc, *N-tert*-butoxycarbonyl; Bz, benzyl; Ac, acetyl; Z, benzyloxycarbonyl; BTpNA, *N*-benzoyltyrosyl *p*-nitroanilide; vdw, van der Waals.

[2] P_1, P_2, etc. refer to inactivator residues amino terminal to the scissile bond, with the residues numbered from the point of cleavage. The corresponding enzyme subsites are designated S_1, S_2, etc. Residues on the carboxyl end of the scissile bond are numbered P_1', P_2', etc. from the point of cleavage, and the corresponding subsites are designated S_1', S_2', etc. (Schechter & Berger, 1967).

0006-2960/94/0433-13792$04.50/0

These facts have led to two proposals from the mechanism of inactivation of serine proteases with peptidyl chloromethanes. Poulos et al. (1976) have proposed that His57 displaces chloride from the α-methylene carbon after hemiketal formation with Ser195 (mechanism I).

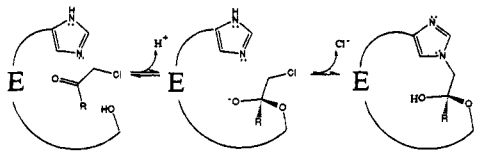

Mechanism I

Powers (1977) has suggested that the hemiketal oxyanion displaces chloride to give an epoxy ether intermediate, which is then attacked by His57 at the less hindered (methylene) carbon to regenerate the hemiketal (mechanism II).

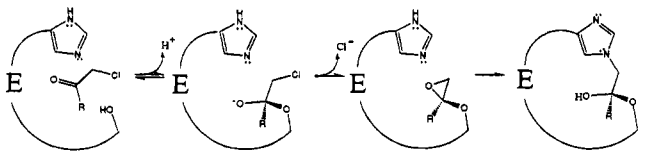

Mechanism II

Since mechanism I predicts a single displacement while mechanism II predicts a double displacement at the chlorocarbon, it occurred to us that the use of a chiral peptidyl α-chloroethane in conjunction with X-ray crystallography could differentiate between the two mechanisms. Here we show that crystalline γ-chymotrypsin reacted with (2*S*)-AcAFCEK at pH 7.0 is alkylated at His57 by the methine

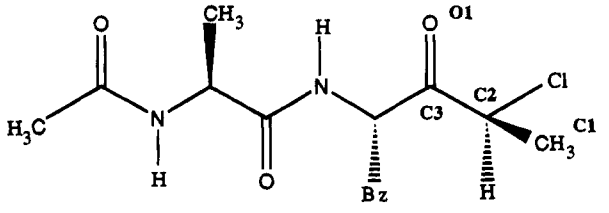

(2*S*)-AcAFCEK

chlorocarbon (C2) of the inactivator and that the absolute configuration of the chiral center in the adduct is S. This result is inconsistent with mechanism I for inactivation of chymotrypsin by this peptidyl chloroethane and is highly supportive of the existence of an epoxy ether on the inactivation pathway.

MATERIALS AND METHODS

α-Chymotrypsin (bovine, type II, 3× crystallized) was obtained from Sigma; ammonium sulfate (ultrapure) was from ICN; cetyltrimethylammonium bromide was from Aldrich; and the phosphate, cacodylate, and acetonitrile were from Fisher Scientific. (2*S*)-AcAFCEK was prepared as described previously (Prorok et al., 1994).

Crystalline Enzyme–Inactivator Complex. α-Chymotrypsin was converted to γ-chymotrypsin as described by Corey et al. (1965). Native crystals were obtained by the method of Cohen et al. (1981). Cocrystals of the enzyme–inactivator complex were obtained in several stages. First, crystals obtained in the 50% saturated ammonium sulfate solution were slowly (over a period of several hours) equilibrated in a 75% ammonium sulfate solution (identical in other components, concentrations, and pH) to stabilize the crystals before adding organic cosolvent. Next, the crystals were slowly equilibrated (over a period of 14 h) with a soaking solution (pH 7.0) consisting of 75% saturated ammonium sulfate, 10 mM potassium phosphate, and 5% (v/v) acetonitrile. Finally, the soaking solution was made 0.5 mM in peptidyl chloroethane, and after 2 days the crystals exposed to the inactivator were transferred to a soaking solution containing 1.0 mM peptidyl chloroethane. Two days later, two small "control" crystals (which were treated identically to the inactivated crystals except that they were not exposed to peptidyl chloroethane) and a single large peptidyl chloroethane-treated crystal which had turned greenish-yellow (indicating inactivation) were separately transferred as ~1-μL aliquots to 50 μL of 1 mM HCl, and their respective activities toward hydrolysis of BTpNA were measured. The enzyme from the control crystals had the same activity as γ-chymotrypsin that had not been crystallized, while the treated enzyme had an activity indistinguishable from the uncatalyzed rate of substrate hydrolysis. The inactivated crystals were soaked for one more day in fresh 1 mM peptidyl chloroethane before a single one (0.4 × 0.4 × 0.6 mm) was mounted in a 0.5-mm quartz capillary.

Table 1

no. of compared reflections	20 852
no. of unique reflections	13 167
completeness of data to 1.8 Å (%)	91
R_{merge}[a] (%)	4.20
resolution range (Å)	20–1.8
R factor[b] (%)	18.8
no. of waters	238
B values (Å^2)	
main chain	5.6
side chains	8.1
inactivator[c]	20.0
waters	22.9
final restraints applied	
σ (bond lengths, Å)	0.020
σ (bond angles, deg)	3.0
σ (planar groups, Å)	0.020
deviations observed	
rms dev (bond lengths, Å)	0.019
rms dev (bond angles, deg)	3.0
rms dev (planar groups, Å)	0.020

[a] $R_{merge} = \Sigma|F_{obs} - F_{avg}|/\Sigma(F_{avg})$. [b] $R = \Sigma|F_o - F_c|/\Sigma(F_o)$. [c] Including N-terminal acetyl group.

Crystallographic Data Collection. Both native and inhibited crystals belong to tetragonal space group $P4_22_12$. The unit cell dimensions ($a = b = 69.5$ Å; $c = 97.6$ Å) indicate that they are isomorphous with each other and that no significant changes in the structure of the unit cell have occurred as a result of complex formation. Intensity data were collected from a single crystal at 4 °C on an *R*-Axis area detector using Cu K_α radiation from a Rigaku RU 200 rotating anode, and the data were reduced with the *R*-Axis program Process (Higashi, 1990). The crystal diffracted to 1.6 Å resolution, but data were only collected to 1.8 Å resolution due to an inability to place the area detector close enough to the crystal to record the highest resolution data. The completeness of the data set to 1.8 Å resolution is 91% (see Table 1).

Crystallographic Refinement. Initial phases were calculated from the coordinates of a refined structure of γ-chymotrypsin soaked with Boc-L-alanyl-L-alanyl-L-phenylalanyl-

O-benzoyl hydroxylamine (1.7 Å resolution with an *R* factor of 17% with σ-weighting for the data) but with the waters and the inhibitor atoms removed. These starting phases gave an initial *R* factor of 27.4% when compared with the data from 20 to 3.0 Å resolution. The difference Fourier electron density map with coefficients $3F_o - 2F_c$ showed inactivator electron density with a distinct bridge to His57 but not to Ser195.

Refinement was carried out by the restrained least squares method with the program TNT (Tronrud et al., 1987). All cycles of refinement were of one iteration each unless stated otherwise. Seven TNT cycles were applied to the data to 3.0 Å resolution, and a map with coefficients $3F_o - 2F_c$ was generated from these loosely constrained coordinates. The map again showed covalent linkage of the inactivator of His57 and not to Ser195, but the precise orientation of the inactivator was still not clear.

Thirty-five TNT cycles were performed on the data to 2.2 Å resolution. The program Waterhunter (S. Sugio, private communication) was then used to place 67 water molecules. At this point, the electron density for the inactivator was clear, and a model (built with Quanta, MSI Corp., Burlington, MA) was built into the electron density at the active site and covalently linked via its C2 methine carbon to the $N^{\epsilon 2}$ of His57 to give the S configuration about C2. The inactivator−His57 linkage was constrained to be 1.44 ± 0.2 Å, with trigonal planar geometry about the His $N^{\epsilon 2}$ atom, as this was shown to be the case in the structure of the model glycoside 1-(tri-*O*-acetyl-α-D-xylopyranosyl)imidazole (Luger et al., 1974). The coordinates for the complex gave an initial *R* factor of 25.9% with excellent geometry.

After four cycles of TNT, it was apparent that the inactivator did not bind in the conformation seen with other peptidyl chloromethane-inactivated serine proteases, with the P_1 side chain squarely in the S_1 pocket and the inactivator chain hydrogen bonded to Ser214 and Gly216. In order to confirm this observation, the inactivator coordinates were deleted, data to 1.8 Å resolution were included, and several cycles of refinement (with individual *B* values refined for the first time) were run to reduce the model bias introduced by the coordinates of the inactivator. Waterhunter was used to add 60 more waters to the model. A difference Fourier electron density map with coefficients $3F_o - 2F_c$ using the coordinates from which the inactivator had been deleted gave a clear electron density in which the inactivator could be positioned unequivocally. Fitting of AcAFCEK in the active site, followed by 16 cycles of refinement, gave an *R* factor of 22.7%.

Forty more waters were added, followed by several cycles of TNT and manual refitting of the entire chain with Frodo (Jones, 1985). Manual refitting included positioning of several side chains and adding and deleting several waters. Eighteen more cycles of TNT (including two with 10 iterations each) and the addition of 24 more waters gave an *R* factor of 19.7%. The first quarter of the protein chain was then manually refitted, followed by TNT refinement of a few cycles of 3−10 iterations each, followed by manual refitting of the second quarter of the chain, followed by TNT refinement, and so on until the whole chain had been examined. Finally, 11 cycles of three iterations each were performed to give a final *R* factor of 18.8%.

To establish that the configuration of the inactivator had been positioned correctly in the active site, an "omit" map was generated: The inactivator atoms were removed from the final structure, and a random change was introduced into the coordinates with the program Shakeup (A. Lavie, personal communication). This new coordinate file was refined for three cycles of three iterations each. Difference Fourier electron density maps with coefficients $2F_o - F_c$ and $F_o - F_c$ showed that the final structure was indeed correct.

As a further test of the validity of the unusual conformation we assigned to the peptidyl chloroethane, we attempted to re-refine the structure as a hemiketal derivative. The inactivator was placed in the active site of the refined structure of native γ-chymotrypsin (Cohen et al., 1981) in exactly the same conformation as was seen for peptidyl chloromethane−serine protease adducts. Native chymotrypsin coordinates were chosen to avoid bias caused by water molecules picked during refinement of the chymotrypsin-peptidyl chloroethane structure. The coordinates of native chymotrypsin were overlaid onto those for the 3.0 Å resolution structure of thrombin inactivated with (D)-FPRCMK (Banner & Hadvary, 1991) using the model-building program Hydra (Dr. R. Hubbard, University of York), and the graphics program Frodo was used to overlay AcAFCEK onto (D)FPRCMK and to connect chymotrypsin residues His57 and Ser195 to the inactivator. Ten active site waters were deleted from the model (hereafter referred to as the hemiketal model), the coordinates were slightly shifted with Shakeup, and five TNT cycles of five iterations each were performed using data to 1.9 Å resolution. As a control, the same procedure was performed on native chymotrypsin containing the inactivator in the conformation seen in this study (hereafter referred to as the ketone model). Both randomly changed coordinate files began with *R* factors of ~35% and ended with *R* factors of ~20.5%, with the ketone model exhibiting better geometry than the hemiketal model. Two facts confirmed the correctness of the ketone model. First, a difference Fourier electron density map with coefficients $2F_o - F_c$ and phases calculated from the hemiketal model had no electron density for the C1 methyl carbon, the C2 methine carbon, or the C3 hemiketal carbon and only poor electron density for the P_1 benzyl group, while the analogous map with phases calculated from the ketone model had continuous electron density from His57 to the P_2 alanine residue except for C_1, which showed an additional patch of electron density indicating the S configuration about C2. Second, refinement of the hemiketal model caused the P_1 amide nitrogen to move out of the hydrogen-bonding distance with Ser214 and caused the hemiketal oxyanion to move out of the oxyanion hole. By contrast, refinement of the ketone model left the placement of the peptidyl chloroethane essentially unchanged, except that the P_2 alanine had not yet reverted to the S configuration after being inverted by the random change in coordinates.

To ensure that the absolute configuration at C2 of AcAFCEK is S, an attempt was made to refine the structure with the R configuration at C2: These 2R coordinates had a random change introduced with Shakeup and were then refined for three cycles of three iterations each. In the resulting model, the C1 methyl group of the peptidyl chloroethane in the R configuration was in poor electron density and was only 2.8 Å from the O^{γ} of Ser195. Furthermore, the His57 $N^{\epsilon 2}$-inactivator C2 bond distance

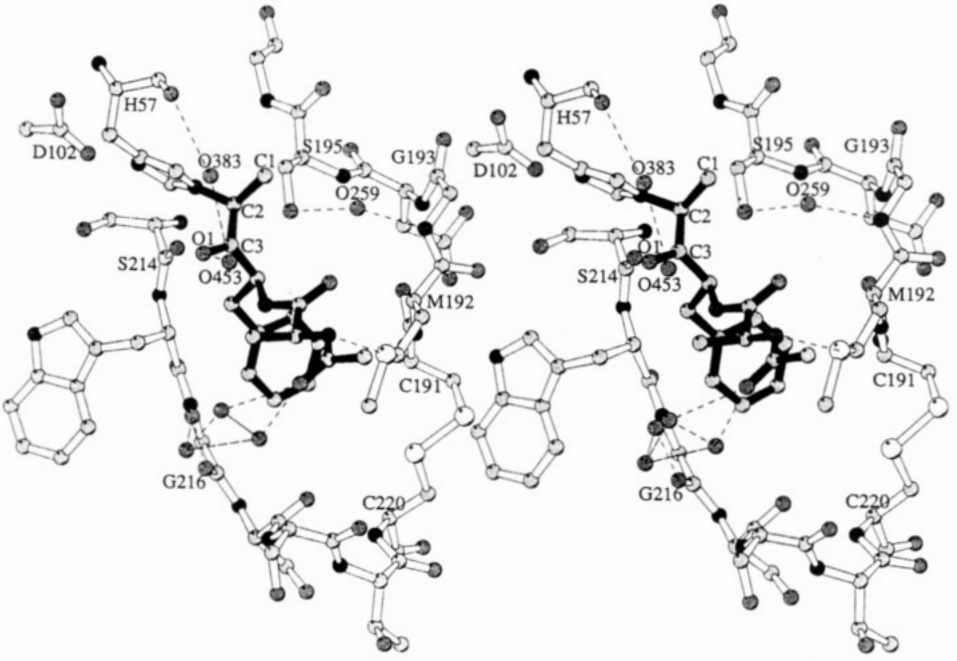

FIGURE 1: Stereoview of the active site region of chymotrypsin inactivated with (2*S*)-AcAFCEK. The view is from the solvent into the S_1 pocket and shows chymotrypsin alkylated at His57 with the S absolute configuration about C2. Residues 189−190 and 225−228 (which define the bottom and part of one side of the pocket) were omitted for clarity. All figures were generated with MOLSCRIPT (Kraulis, 1991).

refined to 1.3 Å. It was concluded that the inactivator is indeed in the 2S configuration.

RESULTS

γ-Chymotrypsin inactivated with (2*S*)-AcAFCEK at pH 7.0 gives a derivative whose C2 methine carbon atom at the alkylated His57 has retained the 2S configuration. The C1 methyl group is 3.4 Å from the C^{β} of Ser195 and 3.5 Å from the O^{γ} of Ser195.

Noncovalent interactions between the inactivator and the enzyme are limited: Neither the P_1 amide nitrogen nor the P_2 carbonyl oxygen, for example, make any hydrogen bonds, and the P_1 benzyl group is not positioned for optimal van der Waals interactions with the S_1 pocket. Nevertheless, the bound inactivator apparently has little mobility as judged by the continuous electron density from His57 to the carbonyl atoms of the acetyl group and the moderately low overall isotropic temperature factor for the inactivator. This is presumably made possible in large part by the three polar interactions that *do* exist between inactivator and protein. Specifically, the P_1 carbonyl oxygen is hydrogen bonded (3.1 Å to Wat453, which is in turn hydrogen bonded to the carbonyl oxygen of His57 via Wat383; the acetyl group is indirectly hydrogen bonded to the carbonyl group of Gly216 via a similar water network; and a dipole−dipole interaction exists between the P_2 amide nitrogen and the sulfur atom of Met192 (the side chain for which exists in two conformations as judged by the "forked" electron density at the C^{β}) (Figure 1).

The binding mode of this inactivator with chymotrypsin is very different from that of any peptidyl chloromethane-inactivated serine protease. First, no hemiketal with Ser195 is seen: the O^{γ} of Ser195 is 3.8 Å from the P_1 carbonyl carbon and is almost directly in line with the axis that the carbonyl group defines.

Second, the P_1 carbonyl oxygen is pointing in a direction almost diametrically opposed to the oxyanion hole defined by the amide nitrogens of Gly193 and Ser195 (Figure 2).

Third, the P_1 amide nitrogen has no hydrogen bonding partners within 3.6 Å. This contrasts sharply with all other serine proteases inactivated with a peptidyl chloromethane: even an inactivator as short as Z-L-lysyl chloromethane complexed to trypsin has the "classic" hydrogen bond between the P_1 amide nitrogen and the carbonyl oxygen of Ser214 (Scott et al., 1986). The small substrate analogue *N*-formyl tryptophan also has this hydrogen bond in the complex with chymotrypsin (Steitz et al., 1969). Unfortunately, it is not known for certain if this hydrogen bond exists between chymotrypsin and Ac-L-alanyl-L-phenylalanyl chloromethane due to crystallographic difficulties encountered by Segal et al. (1971), who could only locate the acetyl-alanyl moiety in difference Fourier maps (Powers, 1977).

Fourth, the P_1 side chain (benzyl group) is only partially in the S_1 hydrophobic subsite defined by residues 189−195 on one side, 214−220 on the other side, and 225−228 along the bottom (Cohen et al., 1981), with the phenyl ring nearly perpendicular to the narrow pocket (Figure 3). The empty portion of the subsite contains a substantial patch of electron density directly in line with and 2.4 Å from the center of the phenyl ring, which has been interpreted as an alternate conformation of the benzyl moiety. Refinement of the phenyl ring in this more "normal" conformation (i.e., parallel to the S_1 pocket) indicated that the perpendicular conformer predominates. The possibility that the electron density represents a water molecule hydrogen bonded to the aromatic group seems less likely since the hydrogen bond distance between a jet-cooled water molecule and benzene is 3.3 Å (Suzuki et al., 1992) and since weakly polar interactions with aromatic groups are no shorter than 3.4 Å for steric reasons (Burley & Petsko, 1986; Levitt & Perutz, 1988).

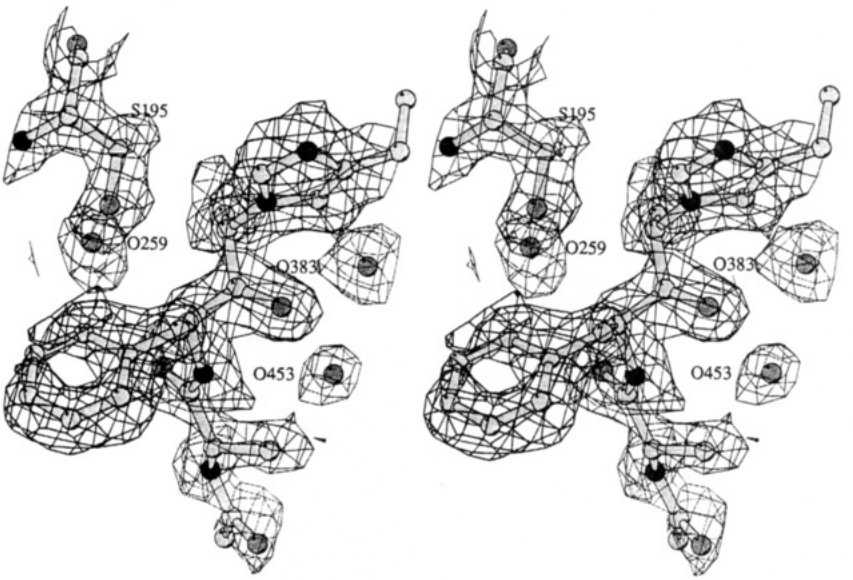

FIGURE 2: Difference Fourier electron density map with coefficients $2F_o - F_c$, contoured at 0.85 σ, using all atoms of the inactivated model. The view is from the active site into the solvent. There is clear electron density for most of the inactivator, and at lower contour levels, the electron density becomes complete for the phenyl ring. The incomplete additional patch of electron density above the phenyl ring may represent a less common conformer of that ring.

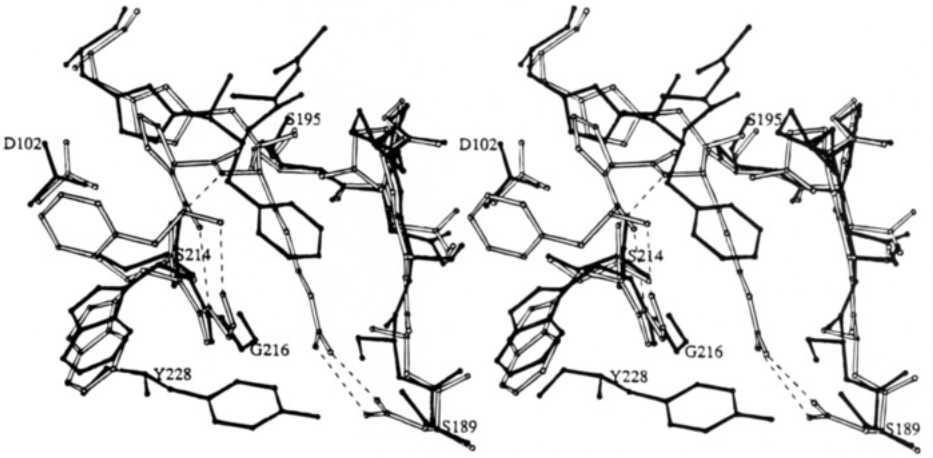

FIGURE 3: Chymotrypsin−AcAFCEK complex (dark bonds) overlaid onto the coordinates of the thrombin−(D)FPRCMK complex (light bonds) (Banner & Hadváry, 1991). This view into the active site is shifted vertically ~90° from Figure 1 to show a cross-section of the S_1 pocket. Residues 217−220 and 225−227 were omitted for clarity. Note that the chymotrypsin inactivator lacks H-bonds to the backbone atoms of Ser214 and Gly216. For comparison, these H-bonds are shown for the thrombin inactivator.

Finally, the alkylated His and P_1 carbonyl group are nearly syn periplanar, with the torsion angle defined by His57 $N^{\epsilon 2}$−C2−C3−O1 equal to 30°. This too is unprecedented for serine proteases inactivated with peptidyl chloromethanes: the alkylated histidine and hemiketal oxyanion are invariably anti periplanar with a torsion angle of 180 ± 30°, with the most common angle being 210°.

DISCUSSION

Chemical Identity of the "Single Displacement" Intermediate. The reaction of γ-chymotrypsin with (2*S*)-AcAFCEK leads to alkylation of His57 with retention of configuration at the chiral center. This fact can best be explained by postulating a double displacement mechanism (where each displacement involves an inversion at C2) in which the single displacement intermediate is the Ser195−epoxy ether adduct (mechanism II). Such an intermediate is known from solution studies to be chemically competent in the transformation of α-chloro ketones to α-amino ketones (Goyau & Rouessac, 1978; Stevens & Chang, 1962). Less likely candidates for the intermediate are an allylic carbocation (followed by attack of His57 on the face from which chloride was expelled) (De Kimpe & Verhé, 1988), a serine ether, or a sulfonium ion generated from the alkylation of Met192 (Powers, 1977). The mechanisms giving rise to these intermediates all have difficulty accounting for the hemiketal ^{13}C resonance at the P_1 carbonyl carbon (C3) observed during the inactivation of chymotrypsin by (2*S*)-AcAFCEK (see below).

Unusual Conformation of the Bound Inactivator. The structural features mentioned in the Results section—lack of a hemiketal formed with Ser195, orientation of the P_1 carbonyl oxygen away from the oxyanion hole, lack of an H-bond between the P_1 backbone nitrogen and the carbonyl oxygen of Ser214, poor placement of the P_1 sidechain in the S_1 pocket, and nearly syn periplanar arrangement of the alkylated His and the P_1 carbonyl group—occur only with this serine protease−peptidyl chloroalkane adduct. One possible explanation for these unique features is that the lack of a P_3 residue in the inactivator is allowing a nonproductive

Table 2

enzyme	inactivator	pH	k_i (s^{-1})	k_i/K_I (M^{-1} s^{-1})	k_i^{Cl}/k_i^F		$k_i/K_I^{Cl}/k_i/K_I^F$	
plasmin	AFKCMK	7.0[d]	0.0030	3.6×10^3	7.1		21	
plasmin	AFKFMK	7.0[e]	0.00042	1.2×10^2 [a]				
thrombin	(D)FPRCMK	7.3[f]	0.30[b]	8.2×10^6 [b]	200		683	
thrombin	(D)FPRCMK	7.8[g]	0.030[b]	1.2×10^7 [b]	20	87[c]	1000	630[c]
thrombin	(D)FPRCMK	8.0[h]	0.063[b]	2.5×10^6 [b]	42		210	
thrombin	(D)FPRFMK	7.0[e]	0.0015	1.2×10^4 [a]				

[a] The peptidyl fluoromethanes were racemic in the P_1 α-carbon, so the reported values for k_i/K_I were doubled to take into account the concentration of the more active inactivator isomer (assumed to be the L-form isomer). [b] These values for k_i and k_i/K_I were extrapolated to pH 7.0 assuming that k_i has a pH dependence with a $pK_a = 7.0$. [c] Average values. [d] Kettner and Shaw (1978). [e] Angliker et al. (1988). [f] Collen et al. (1982). [g] Hofsteenge et al. (1986). [h] Walker et al. (1985).

mode of binding in the active site. This seems unlikely, however, since Z-L-lysyl chloromethane is able to bind "productively" in the active site of trypsin (Scott et al., 1986). Furthermore, the adduct of Ac-L-alanyl-L-phenylalanyl chloromethane with chymotrypsin was studied (Segal et al., 1971) and, although the electron density was difficult to interpret, it was concluded that this inactivator bound to chymotrypsin in the expected fashion. Similarly, it is unlikely that our result is an artifact of having soaked the inactivator into the crystal instead of having crystallized the inactivated enzyme since Scott et al. (1986) and Segal et al. (1971) inactivated their enzymes in the crystalline state.

What is unique about this study is that it employs a peptidyl chloroethane instead of a peptidyl chloromethane. We believe this peptidyl chloroethane binds in an unusual manner because the steric bulk of the C1 methyl group [van der Waals radius 2.0 Å (Eisenberg & Crothers, 1979)] makes the canonical binding conformation unattainable.

This is clearly the case for an epoxy ether intermediate. The inactivator was modeled into the chymotrypsin active site as the epoxy ether using the (D)FPRCMK–thrombin complex as a template. The C1 carbon in this model is only 2.2 Å from the carbonyl carbon (vdw radius 1.5 Å) of the P_2 alanine residue of the inactivator. This steric clash is less severe in the modeled His57-alkylated Ser195 hemiketal where the C1 methyl group of the peptidyl chloroethane is 2.6 Å from the P_2 carbonyl carbon. By contrast, in the thrombin–peptidyl chloromethane complex, the methylene carbon attached to His43 [His57] is 3.5 Å from the P_2 carbonyl carbon. However, the chymotrypsin–peptidyl chloroethane Ser195 hemiketal adduct probably binds in the "normal" fashion since rotation about the C2–C3 bond should allow the methyl group to avoid the P_2 carbonyl carbon.

Unusual positioning of one portion of an active site-bound inactivator due to constraints imposed by a distant portion of the inactivator (in this case, the C1 methyl group) is not without precedent. For example, poor placement of a benzyl group in the S_1 pocket has been observed in chymotrypsin inactivated with 3-benzyl-6-chloro-2-pyrone (Ringe et al., 1986) and is attributed to a compensating favorable salt bridge between the inactivator carboxylate and His57. Similarly, the structure of chymotrypsin inactivated with a *p*-nitrophenylcinnamate shows the carbonyl group of the Ser195–acyl adduct to be pointing away from the oxyanion hole due to the steric constraints of the rigid cinnamoyl group (Stoddard et al., 1990).

It is argued that epoxy ether formation from the normally bound tetrahedral intermediate causes the C1 methyl group to sweep next to the P_2 carbonyl carbon, which causes the inactivator chain to break its hydrogen bond with Ser214 and to dislodge the P_1 benzyl group from its snug fit in the S_1 pocket. This unusually oriented epoxy ether (relative to the presumed conformation adopted by epoxy ethers derived from peptidyl chloromethanes) is then believed to be attacked by His57 to generate a hemiketal adduct with Ser195, which cannot relax to the canonical conformation due to continuing (albeit lessened) close contact of the C1 methyl group with the rest of the inactivator chain. This unstable His57-alkylated Ser195–hemiketal adduct then collapses to expel Ser195, and the change from sp^3 to sp^2 hybridization about C3 causes the inactivator chain to rotate about the C2–C3 bond such that the P_1 carbonyl oxygen is pointing diametrically opposite the oxyanion hole.

This model for the origin of the unusual conformation seen in the chymotrypsin–peptidyl chloroethane adduct is consistent with the observation that chymotrypsin inactivated with ^{13}C-C3-labeled (2*S*)-AcAFCEK, followed by gel filtration to completely remove the unreacted peptidyl chloroethane, gives NMR peaks both at 103 ppm (indicative of a hemiketal at C3) and at 208 ppm (indicative of a carbonyl carbon at C3) 24 h after inactivation (data not shown). The observed resonance at 103 ppm is not caused by a long-lived epoxy ether intermediate, because the relevant carbon in this class of compounds gives a ^{13}C chemical shift of 91–94 ppm (De Kimpe et al., 1983; De Buyck et al., 1982), which when corrected for the substituents present in the enzyme-bound intermediate should be 88–91 ppm (Johnson & Jankowski, 1972).

Mechanism of Inactivation by Peptidyl Chloromethanes. A reevaluation of the available kinetic data on serine protease inactivation by peptide-derived α-halo ketones seems appropriate in light of the probable existence of an epoxy ether intermediate on the inactivation pathway. Of particular importance are the data on serine protease inactivation by peptidyl halomethanes with fluoride and chloride as the leaving group (Table 2). These data indicate that the leaving group effect is only *partially* expressed in k_i (the first-order rate constant for inactivation, obtained under conditions of saturating inactivator) but may or may not be fully expressed in k_i/K_I (the second-order rate constant for inactivation, obtained under conditions in which most of the enzyme has no bound form of the inactivator), depending on the peptidyl halomethane–enzyme pair. The maximal Cl/F leaving group effect for conversion of the enzyme-bound tetrahedral intermediate to the epoxy ether is assumed to be about 700, since ring closure of the 2-chloroethoxide anion to form ethylene oxide is 700 times faster than ring closure of the 2-fluoroethoxide anion (McCabe & Warner, 1948; Knipe, 1973).

Scheme 1

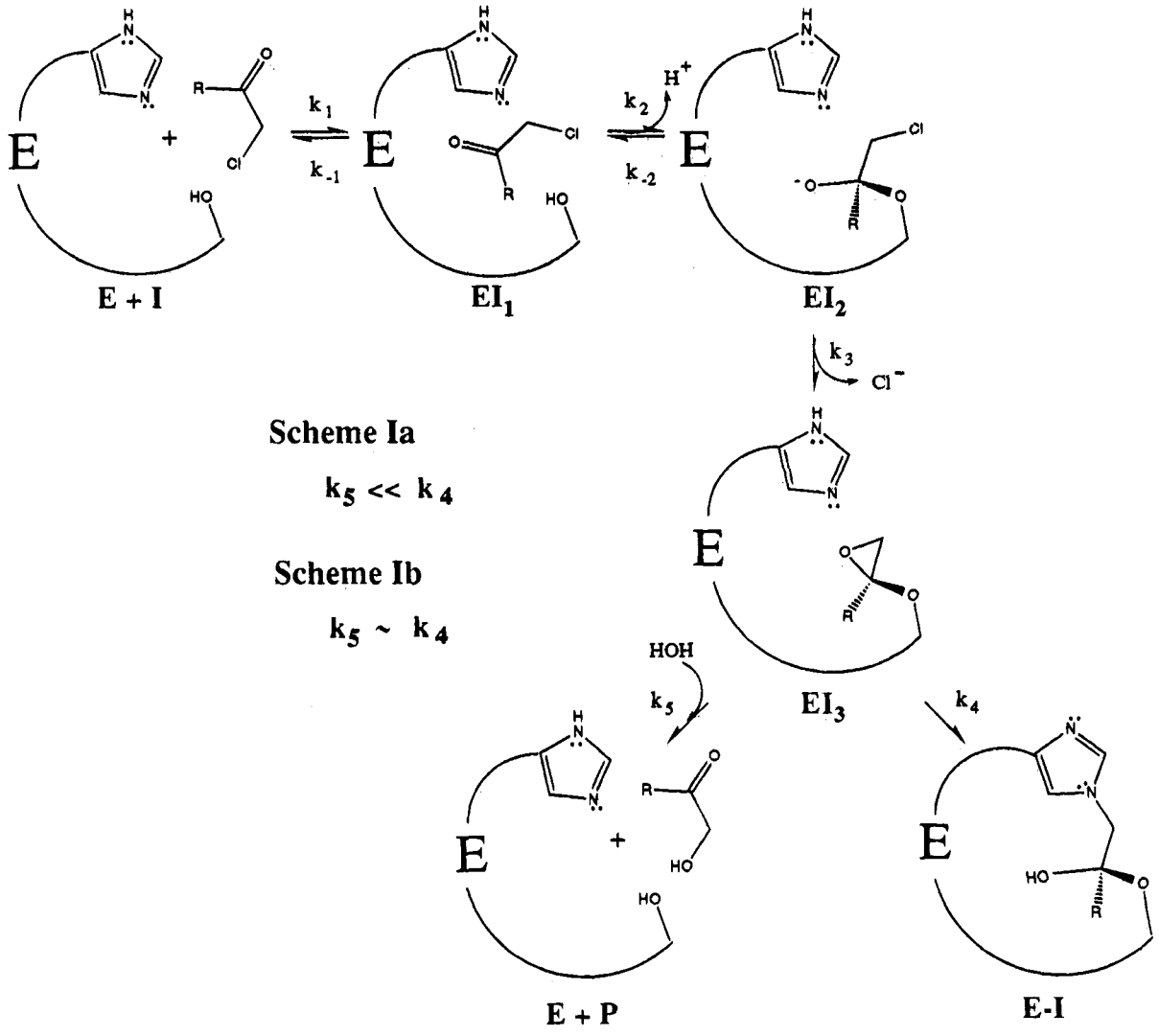

The use of leaving group effects on k_i and k_i/K_I to infer which step(s) on the inactivation pathway are rate-limiting (i.e., have the highest energy transition states and therefore determine k_i/K_I) and which steps have the largest barriers (i.e., determine k_i) relies on two assumptions. It is assumed that the first step significantly influenced by the identity of the leaving group is epoxy ether formation from the tetrahedral intermediate and that epoxy ether formation is irreversible, with rapid escape of halide from the active site relative to halide attack at the epoxy ether to regenerate the hemiketal.

There is evidence that the identity of the halogen significantly influences neither the rate of binding of the (active) ketone form of the inactivator nor the Michaelis complex–hemiketal equilibrium. The linear free energy relationship for the ketone/hydrate equilibrium (Greenzaid et al., 1966) predicts that peptidyl fluoromethanes and peptidyl chloromethanes are hydrated to similar extents [40% and 25%, respectively, as calculated from the σ^* values given by Perrin et al. (1981)], and this prediction has been experimentally confirmed for simple fluoro- and chloromethyl ketones (Greenzaid et al., 1966; Burkey & Fahey, 1983). This argument assumes that formation of the tetrahedral intermediate by serine and its breakdown in the active site have a similar sensitivity to changes in the α-halomethyl group as does hydrate formation and breakdown by bulk water. The fact that chlorine is larger than fluorine [vdw radii 1.80 and 1.35 Å, respectively (Eisenberg & Crothers, 1979)] is not believed to influence any step in the inactivation pathway since the conformation of chymotrypsin-bound Ac-L-leucyl-L-phenylalanyl trifluoromethane is identical to that of serine proteases alkylated with peptidyl chloromethanes (except that His57 is not alkylated), with at least 3.3 Å separating the fluorine atoms from the nearest protein atoms (Brady et al., 1990).

Finally, support for the assumption of irreversible epoxy ether formation comes from the fact that k_i/K_I for inactivation of chymotrypsin by TPCK does not decrease as the buffer NaCl concentration is raised to 1 M. In fact, k_i/K_I increases by the same relative amount with increasing chloride as does k_{cat}/K_M for BTpNA hydrolysis (data not shown).

Thus, the simplest mechanism for inactivation is that the epoxy ether intermediate is quantitatively converted to the His57 alkylated species as shown in Scheme 1a, in which I is the halomethyl ketone, EI_1 is the Michaelis complex, EI_2 is the tetrahedral intermediate, EI_3 is the epoxy ether, and E-I is the His57-alkylated Ser195–hemiketal adduct. Since, in this scheme, EI_3 is an irreversibly dead form of the enzyme (i.e., water cannot react with the epoxy ether), EI_2 and E-I

are experimentally indistinguishable, and k_4 is not observed. The expression for k_i is then given by

$$k_i = k_2k_3/(k_2 + k_{-2} + k_3)$$

(Stein & Trainor, 1986). The rate constant for hemiketal formation, k_2, is greater than 1000 s^{-1} since acyl−enzyme formation from an ester substrate proceeds at least this rapidly (Hess et al., 1970). The rate constant for epoxy ether formation, k_3, is assumed to be much slower than this since ring closure of 2-chloro-1,1-diethyl ethoxide to the epoxide at 25 °C in aqueous solution occurs with a rate constant of ~80 s^{-1} (Streitweiser, 1962). By assuming that $k_2 > k_3$, the expression for k_i simplifies to

$$k_i = k_2k_3/(k_2 + k_{-2})$$

where $k_2/(k_2 + k_{-2})$ is not significantly sensitive to the identity of the leaving group. It follows, then, that since k_i is wholly sensitive to a change in k_3 for Scheme 1a, this mechanism cannot account for all of the leaving group data because it predicts a maximal leaving group effect in k_i, and such an effect is not seen for either peptidyl halomethane.

Since Prorok et al. (1994) have shown that Z-L-alanyl-glycyl-L-phenylalanyl chloromethane is enzymatically converted to chymotrypsin to the peptidyl hydroxymethane with a partitioning ratio of 1:3.6 turnover to inactivation events, one can imagine that this occurs in all reactions of peptidyl chloromethanes with serine proteases as in Scheme 1b. In this scheme, k_i/K_I is not a function of k_4 per se, since k_4 occurs after the first irreversible step, k_3. Rather, k_i/K_I is the product of the second-order rate constant for epoxy ether formation (equivalent to the expression for k_i/K_I in Scheme 1a) and the fraction of forward partitioning of the epoxy ether to give irreversible inactivation, $k_4/(k_4 + k_5)$. Since this forward partitioning is the same for a given peptidyl halomethane−enzyme pair, regardless of the identity of the leaving group, rescue of a fraction of the enzyme epoxy ether by solvent cannot mask the sensitivity of k_i/K_I to a change in k_3. A submaximal leaving group effect in k_i/K_I can be explained only in terms of an earlier step being partially or wholly rate-limiting relative to k_3. Therefore, Scheme 1b is consistent with the leaving group effects in k_i/K_I if $k_{-2} \sim k_3$ for the plasmin−peptidyl halomethane system (so that the transition states for hemiketal formation and epoxy ether formation each partially determine k_i/K_I) and $k_{-2} > k_3$ for the thrombin−peptidyl halomethane system.

By contrast, k_i in Scheme 1b is a function of k_4 (which is independent of k_5) since k_i is determined by all rate constants after inactivator binding (Waley, 1985). Therefore, although the barrier for attack of histidine on the epoxy ether is the same for a given peptidyl−halomethane enzyme pair, k_4 will partially or wholly mask the sensitivity of k_i to a change in k_3, if k_4 is similar to or smaller than k_3. Thus, Scheme 1b is consistent with the leaving group effects in k_i if k_3 and k_4 both have large barriers which each partially determine k_i. The rate constants k_3 and k_4 are each probably less than 1 s^{-1} since k_i is almost always less than 0.1 s^{-1} at pH 7.0 (Markland et al., 1981; Kettner & Shaw, 1978).

In conclusion, Scheme 1a is inconsistent with the kinetic data, while Scheme 1b is consistent with them. It is interesting that epoxy ether formation from peptidyl chloromethanes is so slow on these enzymes, since the rate constant for ring closure of 2-chloro-1,1-diethyl ethoxide anion free in solution is much faster—approximately 80 s^{-1} (Streitweiser, 1962). This may reflect in part the lowered basicity of the enzyme-bound hemiketal oxyanion [pK_a depressed by at least 4 units relative to the solution pK_a (Brady et al., 1989)] due to the presence of the oxyanion hole. There may also be steric constraints imposed by the active site geometry which slow the conversion of the hemiketal to the epoxy ether.

Peptidyl chloromethanes have been characterized as affinity labels, inherently reactive molecules dependent only on formation of a noncovalent enzyme−inactivator complex to effect inactivation (Powers, 1977). The second group of irreversible inactivators, the so-called k_{cat} inhibitors or suicide substrates, are relatively unreactive molecules converted to a reactive form by the enzyme's catalytic machinery. Once activated, they partition between escape from the active site and irreversible inactivation of the enzyme (Rando, 1974). In this paper and in Prorok et al. (1994), we show that inactivation of serine proteases by peptidyl chloroalkanes proceeds by an intermediate which partitions between escape (in chemically modified form) from the active site and irreversible inactivation of the enzyme. The distinction between affinity labels and suicide substrates will inevitably include an area of overlap as our understanding of enzyme inactivation mechanisms becomes more detailed.

ACKNOWLEDGMENT

We are grateful to Dr. W. P. Jencks and Chris Borysenko for helpful discussions and to Dan and Ezra Peisach for guidance in the preparation of the figures.

REFERENCES

Angliker, H., Wikström, P., Rauber, P., Stone, S., & Shaw, E. (1988) *Biochem. J. 256*, 481−486.
Angliker, H., Wikström, P., Shaw, E., Brenner, C., & Fuller, R. S. (1993) *Biochem. J. 293*, 75−81.
Banner, D. W., & Hadváry, P. (1991) *J. Biol. Chem. 266*, 20085−20093.
Brady, K., Liang, T.-C., & Abeles, R. H. (1989) *Biochemistry 28*, 9066−9070.
Brady, K., Wei, A., Ringe, D., & Abeles, R. H. (1990) *Biochemistry 29*, 7600−7607.
Burkey, T. J., & Fahey, R. C. (1983) *J. Am. Chem. Soc. 105*, 868−871.
Burley, S. K., & Petsko, G. A. (1986) *FEBS Lett. 203*, 139−143.
Cohen, G. H., Silverton, E. W., & Davies, D. R. (1981) *J. Mol. Biol. 148*, 449−479.
Collen, D., Matsuo, O., Stassen, J. M., Kettner, C., & Shaw, E. (1982) *J. Lab. Clin. Med. 99*, 76−93.
Corey, R. B., Battfay, O., Brueckner, D. A., & Mark, F. G. (1965) *Biochim. Biophys. Acta 94*, 535−545.
De Buyck, L., Dewaele, M., De Kimpe, N., Verhé, R., & Schamp, N. (1982) *Bull. Soc. Chim. Belg. 91*, 695−706.
De Kimpe, N., & Verhé, R. (1988) *The chemistry of α-haloketones, α-haloaldehydes, and α-haloimines*, John Wiley & Sons, New York.
De Kimpe, N., De Buyck, L., Verhé, R., & Schamp, N. (1983) *Chem. Ber. 116*, 3631−3636.
Eisenberg, D., & Crothers, D. (1979) *Physical Chemistry with Applications to the Life Sciences*, The Benjamin/Cummings

Publishing Co., Inc., Menlo Park, CA.
Finucane, M. D., & Malthouse, J. P. G. (1992) *Biochem. J. 286*, 889−900.
Goyau, B., & Rouessac, F. (1978) *Bull. Soc. Chim. Fr.* 590−592.
Greenzaid, P., Luz, Z., & Samuel, D. (1967) *J. Am. Chem. Soc. 89*, 749−756.
Hallenberger, S., Bosch, V., Angliker, H., Shaw, E., Klenk, H.-D., & Garten, W. (1992) *Nature 360*, 358−361.
Hess, G. P., McConn, J., Ku, E., & McConkey, G. (1970) *Philos. Trans. R. Soc. London B257*, 89−104.
Higashi, T. (1990) *A Program for Indexing and Processing R-AXIS IIC Imaging Plate Data*, Rigaku Corp., Tokyo.
Hofsteenge, J., Taguchi, H., & Stone, S. R. (1986) *Biochem. J. 237*, 243−251.
Johnson, L. F., & Jankowski, W. C. (1972) *Carbon-13 NMR Spectra*, John Wiley & Sons, New York.
Jones, T. A. (1985) *Methods Enzymol. 115*, 157−171.
Kettner, C., & Shaw, E. (1978) *Biochemistry 17*, 4778−4784.
Knipe, A. C. (1973) *J. Chem. Soc. Perkin Trans. 2* 589−595.
Kraulis, P. J. (1991) *J. Appl. Crystallogr. 24*, 946−950.
Levitt, M., & Perutz, M. F. (1988) *J. Mol. Biol. 201*, 751−754.
Luger, P., Kothe, G., & Paulsen, H. (1974) *Chem. Ber. 107*, 2626−2634.
Markland, F. S., Kettner, C., Shaw, E., & Bajwa, S. S. (1981) *Biochem. Biophys. Res. Commun. 102*, 1302−1309.
McCabe, C. L., & Warner, J. C. (1948) *J. Am. Chem. Soc. 70*, 4031−4034.
Perrin, D. D., Dempsey, B., & Serjeant, E. P. (1981) *pK_a Prediction for Organic Acids and Bases*, Chapman & Hall, Ltd., London.
Poulos, T. L., Alden, R. A., Freer, S. T., Birktoft, J. J., & Kraut, J. (1976) *J. Biol. Chem. 251*, 1097−1103.
Powers, J. C. (1977) *Chem. Biochem. Amino Acids, Pept., Proteins 4*, 65−178.
Prorok, M., Albeck, A., Foxman, B. M., & Abeles, R. H. (1994) *Biochemistry 33*, 9784−9790.
Rando, R. R. (1974) *Science 185*, 320−324.
Ringe, D., Mottonen, J. M., Gelb, M. H., & Abeles, R. H. (1986) *Biochemistry 25*, 5633−5638.
Schechter, I., & Berger, A. (1967) *Biochem. Biophys. Res. Commun. 27*, 157−162.
Scott, A. I., MacKenzie, N. E., Malthouse, J. P. G., Primrose, W. U., Fagerness, P. E., Brisson, A., Qi, L. Z., Bode, W., Carter, C. M., & Jang, Y. J. (1986) *Tetrahedron 42*, 3269−3276.
Segal, D. M., Powers, J. C., Cohen, G. H., Davies, D. R., & Wilcox, P. E. (1971) *Biochemistry 10*, 3728−3738.
Stein, R. L., & Trainor, D. A. (1986) *Biochemistry 25*, 5414−5419.
Steitz, T. A., Henderson, R., & Blow, D. M. (1969) *J. Mol. Biol. 46*, 337−348.
Stevens, C. L., & Chang, C. H. (1962) *J. Org. Chem. 27*, 4392−4396.
Stoddard, B. L., Bruhnke, J., Porter, N., Ringe, D., & Petsko, G. A. (1990) *Biochemistry 29*, 4871−4879.
Streitwieser, A., Jr. (1962) *Solvolytic Displacement Mechanisms*, McGraw-Hill, New York.
Suzuki, S., Green, P. G., Bumgarner, R. E., Dasgupta, S., Goddard, W. A., III, & Blake, G. A. (1992) *Science 257*, 942−945.
Tronrud, D. E., Ten Eyck, L. F., & Matthews, B. W. (1987) *Acta Crystallogr., Sect. A A43*, 489−501.
Waley, S. G. (1985) *Biochem. J. 227*, 843−849.
Walker, B., Wikstrom, P., & Shaw, E. (1985) *Biochem. J. 230*, 645−650.
Weiner, H., White, W. N., Hoare, D. G., Koshland, D. E., Jr. (1966) *J. Am. Chem. Soc. 88*, 3851−3859.